

The phonon boundary scattering cross section at disordered crystalline interfaces: a simple model

D Kechrakos†

Department of Theoretical Physics, University of Oxford, 1 Keble Road, Oxford
OX1 3NP, UK

Received 18 September 1989, in final form 2 November 1989

Abstract. We present a formalism for the study of the effects of alloy disorder at crystalline interfaces on the phonon boundary scattering cross section. The disordered region is treated within the coherent potential approximation adapted to the interface geometry. The formalism is based on *t*-matrix scattering theory and allows for separation of the coherent and incoherent parts of the reflection and transmission channels. The theory is developed for a single-phonon-branch model and numerical results are presented for a simple cubic interface.

1. Introduction

The problem of phonon scattering at crystalline interfaces has attracted considerable theoretical and experimental interest in the past years mainly in connection with the perpendicular heat transport between two solids in contact (Anderson 1981). Recent advances in high-frequency phonon generation and detection techniques (Wybourne and Wigmore 1988) have revived theoretical interest in the subject as they gave more ground to the microscopic (atomic scale) descriptions of the scattering process over the macroscopic treatments within the elasticity theory framework.

In this direction, some authors in the past (Steinbruchel 1976, Arimitsu *et al* 1984, Jex 1986) have implemented simple one-dimensional (1D) models to investigate the qualitative behaviour of the phonon boundary scattering cross section at frequencies well within the dispersive regime. Studies on more realistic 3D models of semiconductor heterojunctions have also appeared (Streib and Mahler 1987, Deans and Inkson 1989). The conclusion from these studies is that the dispersion effects decrease the transmission across the boundary and cause a very strong dependence of the cross section on the phonon frequency. The sensitivity of the cross sections on the detailed atomic structure at the interface region has also been demonstrated.

A common characteristic of the above models is that either they cannot (1D models) or they do not (3D models) allow for deviations from perfect crystallinity at the interface region, which is a well known feature of all real interfaces. For example, dangling bonds, misfit dislocations, chemical impurities, interdiffusion, etc, are all candidates for breaking the 2D periodicity parallel to the boundary plane. The major feature introduced by the presence of interface disorder is the coupling of phonons with different wavevector

† Present address: Department of Physics, University of Exeter, Stocker Road, Exeter EX4 4QL, UK.

components parallel to the boundary, which gives rise to *diffuse* or *incoherent* scattering. The opening of the diffuse scattering channel modifies drastically the energy flux across the boundary and many experiments in the past have demonstrated this effect (Anderson 1981).

The problem of phonon scattering at non-planar boundaries has so far been treated quite extensively in the low-frequency regime, where a continuum theory approach is adequate (Ogilvy 1987). However, to our knowledge, no studies of the same problem on a microscopic level exist.

The purpose of our work is, first, to develop an atomic scale calculation scheme for the phonon boundary scattering cross section and, secondly, to incorporate in the same scheme the effects of interface disorder. In particular, we consider the case in which an atomic plane at the interface region between two monatomic crystals is randomly occupied by both types of atoms. We separate the diffuse from the specular contribution to each of the transmitted and reflected channels and study their dependence on the incident and scattered angles, the frequency and the degree of disorder. We show that the interplay of disorder and dispersion effects leads to various features in the scattering coefficients and the angular distribution of the scattered flux. Our formalism is based on the Green function scattering theory of imperfect crystals and random alloys.

In section 2 we present the Green function (GF) treatment of the scattering problem and derive expressions for the reflection and transmission cross sections. The interface with no interdiffused atoms (clean) is treated first to help us establish the notation and clarify the complications introduced by the presence of interface disorder. For the sake of simplicity the whole analysis is presented for a single-phonon-branch model. In section 3 we discuss the numerical results for an interface between two simple cubic crystals and in section 4 we summarise our work and discuss the extension of these ideas to a multibranch model and to other types of interface defects.

2. Theory

2.1. Periodic interface

We describe the formation of a planar interface between two lattice-matched crystals as a localised perturbation in an augmented Hilbert space, which consists of the direct product of the Hilbert spaces of the constituent crystals (Pollman and Pantelides 1980). In practice, this extension of the Hilbert space implies that all vector and matrix quantities entering the calculation should be partitioned as

$$\begin{bmatrix} A \\ B \end{bmatrix} \quad \text{and} \quad \begin{bmatrix} AA & AB \\ BA & BB \end{bmatrix}$$

respectively, where A and B denote the two sides of the interface. In particular, the unperturbed system consists of a pair of 3D non-interacting crystals with GF

$$P = \begin{bmatrix} P_A & 0 \\ 0 & P_B \end{bmatrix} \quad P_s = (\omega^2 - D_s)^{-1} \quad s = A, B \quad (1)$$

where D is the dynamical matrix for the infinite crystal. Let V^{IF} be the perturbing

potential that couples them, creating a pair of identical interfaces, and T^{IF} the corresponding t -matrix

$$T^{\text{IF}} = \begin{bmatrix} T_{\text{AA}}^{\text{IF}} & T_{\text{AB}}^{\text{IF}} \\ T_{\text{BA}}^{\text{IF}} & T_{\text{BB}}^{\text{IF}} \end{bmatrix} = V^{\text{IF}}(I - PV^{\text{IF}})^{-1}. \quad (2)$$

The interface t -matrix includes all the multiple scattering effects of the perturbation potential on the phonons of the two crystals. Furthermore, the eigenstates of the perturbed system are given from the *Lippmann-Schwinger* equation (Economou 1983)

$$u = u^0 + PT^{\text{IF}}u^0$$

where u^0 is an eigenstate of the unperturbed system, describing plane waves striking the interface region. If we assume that the incident wave comes from side A only, then $u_{\text{B}}^0 = 0$ and the last equation provides

$$u_{\text{A}} = u_{\text{A}}^0 + P_{\text{A}}T_{\text{AA}}^{\text{IF}}u_{\text{A}}^0 = u_{\text{A}}^0 + w_{\text{A}} \quad (3)$$

$$u_{\text{B}} = P_{\text{B}}T_{\text{BA}}^{\text{IF}}u_{\text{A}}^0 = w_{\text{B}} \quad (4)$$

where the identification of the reflected (w_{A}) and transmitted (w_{B}) fields has been made. To evaluate the actual scattering amplitudes, the asymptotic behaviour of those fields is required. The conservation of the parallel component of the momentum (k_{p}) of the incident wave, dictated by the 2D periodicity of V^{IF} , implies that we should calculate the asymptotic expansion of equations (3) and (4) in the layer representation. To proceed we restrict ourselves to a single-branch model. For an incident phonon of frequency ω_0 and wavevector $k^0 = (k_{\text{p}}, q^0)$,

$$u_{\text{A}}^0(n'') = \exp(iq^0 n'' d) \quad (5)$$

q^0 being the wavevector component along the interface growth direction, the reflected field on the n th layer reads

$$w_{\text{A}}(n) = \sum_{n', n''} P_{\text{A}}(n, n') T_{\text{AA}}^{\text{IF}}(n', n'') u_{\text{A}}^0(n'') \quad (6)$$

where d is the distance between nearest planes. Notice that we have suppressed the k_{p} dependence in equations (5) and (6). One needs the behaviour of the sum in equation (6) for planes very distant from the interface, i.e. in the limit $|n| \rightarrow \infty$. It is shown in appendix 1 that for a single-branch model

$$P_{\text{A}}(n, n') \underset{|n-n'| \rightarrow \infty}{\sim} -i \frac{\exp[iq^{\text{s}}(n-n')d]}{|\partial \omega_{\text{A}}^2(\mathbf{k})/\partial q|_{\text{s}}} \quad (7)$$

where $k^{\text{s}} = (k_{\text{p}}, q^{\text{s}})$ is the wavevector of the reflected phonon. Substitution of equations (5) and (7) into equation (6) provides the asymptotic expansion of the reflected field

$$w_{\text{A}}(n) \underset{|n| \rightarrow \infty}{\sim} f_{\text{A}}(q^0 \rightarrow q^{\text{s}}) \exp(iq^{\text{s}} n d)$$

where the *reflection amplitude* is given by

$$f_{\text{A}}(q^0 \rightarrow q^{\text{s}}) = \frac{-i}{|\partial \omega_{\text{A}}^2(\mathbf{k})/\partial q|_{\text{s}}} \sum_{n', n''} \exp(-iq^{\text{s}} n' d) T_{\text{AA}}^{\text{IF}}(n', n'') \exp(iq^0 n'' d). \quad (8a)$$

Clearly, far from the interface region, the reflected wave behaves as a bulk phonon of crystal A. In a similar fashion one can obtain for the *transmission amplitude*

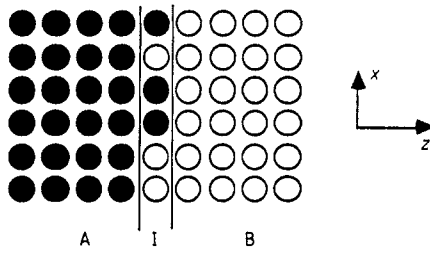


Figure 1. Model of a microscopically rough boundary.

$$f_B(q^0 \rightarrow q^s) = \frac{-i}{|\partial \omega_B^2(\mathbf{k})/\partial q|_s} \sum_{n', n''} \exp(-iq^s n' d) T_{BA}^{IF}(n', n'') \exp(iq^0 n'' d). \quad (8b)$$

The *energy flux* in the z direction carried by the wave $(\omega, \mathbf{k}_p, q)$ with amplitude A_k is

$$J = \omega^2 |A_k|^2 v(q) \quad v(q) = \partial \omega(\mathbf{k})/\partial q$$

and the *power reflection/transmission coefficients* are defined as the ratio of the reflected/transmitted over the incident flux

$$r_{AA}(q^0 \rightarrow q^s) = |f_A(q^0 \rightarrow q^s)|^2 |v_A(q^s)/v_A(q^0)| \quad (9a)$$

$$t_{BA}(q^0 \rightarrow q^s) = |f_B(q^0 \rightarrow q^s)|^2 |v_B(q^s)/v_A(q^0)|. \quad (9b)$$

These satisfy the following *reciprocity relations* (Schiff 1955):

$$r_{AA}(q^0 \rightarrow q^s) = r_{AA}(-q^s \rightarrow -q^0) \quad \mathbf{k}_p = \text{fixed} \quad (10a)$$

$$t_{BA}(q^0 \rightarrow q^s) = t_{AB}(-q^s \rightarrow -q^0) \quad \mathbf{k}_p = \text{fixed} \quad (10b)$$

and the *flux conservation law*:

$$r_{AA}(q^0) + t_{BA}(q^0) = 1 \quad \mathbf{k}_p = \text{fixed}. \quad (10c)$$

Equations (8) and (9) include all the information about the elastic phonon scattering at a periodic crystal interface for the case of a single-branch lattice dynamics model. Notice, also, that equation (8) is equally applicable to the case in which one or both of the incoming and outgoing modes is non-propagating (evanescent), characterised by a complex q ; therefore, it can be used to investigate the existence of interface localised modes, since the latter can be thought of as coupled evanescent modes of the two crystals (Deans and Inkson 1989).

We conclude this section with the following remark. Our scattering theory method for calculating the scattering amplitude of a particular mode does not require explicit knowledge of *all* the modes of the two crystals, but simply those directly involved in the scattering process, and we believe that this is the major advantage of the t -matrix formulation of the boundary scattering problem over the alternative 'field matching' techniques (Streib and Mahler 1987, Deans and Inkson 1989).

2.2. Disordered interface

Consider next an interface A–B between two monatomic lattice-matched crystals, which is geometrically abrupt except for an atomic monolayer right at the interface region randomly occupied by atoms of both crystals ($A_{1-c}B_c$). The profile of this interface is shown in figure 1.

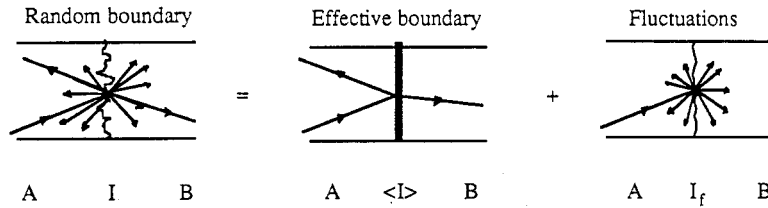


Figure 2. Analysis of the scattering process to a specular and a diffuse component.

Assume that the disordered region arises from diffusion of B atoms into the first planes of crystal A. When a phonon A with wavevector k^i enters the interface region (I), it is scattered off by two potentials, (i) the clean-interface potential and (ii) the random potential caused by the random distribution of B atoms. The former changes the phase (i.e. wavevector) of the incident phonon in a well defined way because of its 2D symmetry; while the latter causes a random change to the phonon phase. We can simplify this picture by considering the scattering off the disordered layer as a sum of two *non-interfering* processes (figure 2), as follows.

(i) Scattering off the underlying effective medium, characterised by a uniform complex potential. This process causes strong interference effects between the waves emerging from the various scattering centres (B atoms) and the cumulative effect of those is that some preferable outgoing directions arise. Furthermore, because the effective-medium potential has the same periodicity as the clean-interface potential, by considering the scattering off the sum of the two potentials the scattering pattern is not changed, but only the relative intensities of the scattered waves. The total scattering process is described as *coherent* and it gives rise to the *specular* phonon beam.

(ii) Scattering off the fluctuations from the effective medium. These scattering events are absolutely independent, since all possible interference effects have already been included in the scattering off the effective medium. The final outcome of this process is a wave with a random phase and therefore no preferable outgoing direction. This process is described as *incoherent* and it gives rise to the *diffuse* phonon beam.

We proceed with the mathematical description of these processes. The uniform potential describing the effective medium is given by the self-energy operator Σ , which is determined by standard random alloys techniques (Elliott *et al* 1974). In particular, in the coherent potential approximation (CPA) the self-energy is adjusted so that the alloy fluctuations away from the effective medium produce zero extra scattering of the excitations. Thus, if G is the clean interface GF and \bar{G} the GF of the interface with the random monolayer replaced by an effective periodic medium, these are related by

$$\bar{G} = G + G\Sigma\bar{G}. \quad (11)$$

The t -matrix describing the scattering off the alloy fluctuations reads

$$T^t = V^t(I - \bar{G}V^t)^{-1} \quad V^t = V^r - \Sigma$$

where V^r is the random potential in the disordered layer. On average, the above equation provides

$$\langle T^f \rangle = (1 - c) \frac{V_A - \Sigma}{I - (V_A - \Sigma)\bar{G}} + c \frac{V_B - \Sigma}{I - (V_B - \Sigma)\bar{G}} = (1 - c)T_A + cT_B. \quad (12)$$

The standard CPA equation reads

$$\langle T^f \rangle = 0. \quad (13)$$

Equations (11)–(13) constitute a self-consistent set that can, in principle, be solved by iteration to provide the self-energy. In practice, the convergence of a simple iteration scheme for equation (13) is very poor and the scheme (Chen 1973)

$$\Sigma' = \Sigma + \langle T^f \rangle (I + \langle T^f \rangle \bar{G})$$

is used instead, with the initial value

$$\Sigma^{(0)} = \langle V \rangle = (1 - c)V_A + cV_B.$$

The total potential that scatters the phonons at the interface region can be written as a sum of three terms:

$$V = V^{IF} + \Sigma + V^f.$$

We define the *effective interface potential* as

$$U = V^{IF} + \Sigma$$

and thus

$$V = U + V^f. \quad (14)$$

Equation (14) clearly shows that the total potential that scatters the incident phonons consists of two components, the first of which has the 2D periodicity of the underlying lattice plane and therefore preserves the k_p component of the incident phonons, and the second of which has a point symmetry and does not preserve the k_p component. Consequently, the corresponding scattering t -matrix can be written as

$$T = \bar{T} + \delta T \quad (15)$$

where \bar{T} describes the multiple scattering off the effective interface potential and δT the corrections arising from the fluctuation potential. In particular,

$$\bar{T} = U(I - PU)^{-1} \quad (16)$$

and after some little algebra

$$\delta T = (I + \bar{T}P)T^f(I + P\bar{T}). \quad (17)$$

The Lippmann–Schwinger equation for the total fields reads

$$u = u^0 + P\bar{T}u^0 + P\delta Tu^0 = u^0 + \bar{u} + GT^f\bar{u} = u^0 + \bar{u} + u^f. \quad (18)$$

The second term on the right-hand side of equation (18) is the *coherent* or *specular field* (\bar{u}) and the third term the *incoherent* or *diffuse field* (u^f). As in the previous section, the scattering amplitudes will be determined from the asymptotic expansion of equation (18).

For the coherent field one proceeds as in the case of a clean interface (see section 1) and the final expressions can be obtained from equations (8) and (9) with the replacement

$$T^{IF} \rightarrow \bar{T}.$$

For the incoherent field, we leave the details of the calculation for appendix 2, and we give here the asymptotic expansion for a single-branch model

$$u_i^f(l) \sim \sum_{|n| \rightarrow \infty} \sum_{k_p^s} h_i(k_p^0 \rightarrow k_p^s) \exp(ik^s \cdot l) \quad i = A, B$$

where $l = (l_p, nd)$ denotes a lattice site of the interface system and $k^0 = (k_p^0, q^0)$ and $k^s = (k_p^s, q^s)$ are the incident and scattered wavevectors, respectively. The above equation shows that the diffuse field away from the disordered plane is a linear superposition of bulk phonons propagating in all possible directions consistent with frequency conservation. Furthermore, the diffuse scattering amplitude h is a random quantity, and therefore the average cross sections should be proportional to the configurational average $\langle |h|^2 \rangle$. In particular, we define the following cross sections for the diffuse process:

(i) The *angular distribution of the reflected/transmitted flux* of an incident phonon (ω, k^0) is

$$r_{AA}^d(k_p^0 \rightarrow k_p^s) = \langle |h_A(k_p^0 \rightarrow k_p^s)|^2 \rangle |v_A(q^s)/v_A(q^0)| \quad (19a)$$

$$t_{BA}^d(k_p^0 \rightarrow k_p^s) = \langle |h_B(k_p^0 \rightarrow k_p^s)|^2 \rangle |v_B(q^s)/v_A(q^0)| \quad (19b)$$

which satisfy the reciprocity relations (Schiff 1955):

$$r_{AA}^d(k^0 \rightarrow k^s) = r_{AA}^d(-k^s \rightarrow -k^0) \quad (20a)$$

$$t_{BA}^d(k^0 \rightarrow k^s) = t_{BA}^d(-k^s \rightarrow -k^0). \quad (20b)$$

(ii) The *power reflection/transmission coefficient* of an incident phonon (ω, k^0) is

$$R_{AA}^d(k^0; \omega) = \sum_{k_p^s} r_{AA}^d(k_p^0 \rightarrow k_p^s) \quad (21a)$$

$$T_{BA}^d(k^0; \omega) = \sum_{k_p^s} t_{BA}^d(k_p^0 \rightarrow k_p^s). \quad (21b)$$

The *flux conservation* requires that for a given incident phonon (ω, k^0)

$$R_{AA}^{sp}(q^0) + T_{BA}^{sp}(q^0) + R_{AA}^d(k_p^0) + T_{BA}^d(k_p^0) = 1 \quad (22)$$

where the superscript 'sp' indicates the specular components.

3. Application

3.1. The interface model

In order to illustrate the type of results obtained from the previously derived expressions for the scattering cross sections, we consider a (001) interface between two lattice-matched simple cubic crystals with first-nearest-neighbour interactions. In this lattice model (Montroll and Potts 1956) the three directions of motion are completely decoupled, and thus the 1D theory presented in section 2 is directly applicable. For simplicity we assume that the force constants for motion parallel and perpendicular to the bond

are both equal to λ , and therefore the bulk phonon band structure consists of three degenerate branches

$$\omega^2(\mathbf{k}) = (2\lambda/m)(3 - \cos k_x - \cos k_y - \cos k_z) \quad \text{lattice constant } a = 1.$$

The interface potential for the bicrystal reads

$$V^{\text{IF}} = \begin{bmatrix} Q_{\text{AIF}} & Q_{\text{A}} & 0 & Q_{\text{IF}} \\ Q_{\text{A}} & Q_{\text{AIF}} & Q_{\text{IF}} & 0 \\ 0 & Q_{\text{IF}} & Q_{\text{BIF}} & Q_{\text{B}} \\ Q_{\text{IF}} & 0 & Q_{\text{B}} & Q_{\text{BIF}} \end{bmatrix}$$

where

$$Q_{\text{A}} = \frac{\lambda_{\text{A}}}{m_{\text{A}}} \quad Q_{\text{AIF}} = \frac{-\lambda_{\text{A}} + \lambda_{\text{IF}}}{m_{\text{A}}} \quad Q_{\text{B}} = \frac{\lambda_{\text{B}}}{m_{\text{B}}} \quad Q_{\text{BIF}} = \frac{-\lambda_{\text{B}} + \lambda_{\text{BIF}}}{m_{\text{B}}} \\ \times Q_{\text{IF}} = \frac{\lambda_{\text{IF}}}{(m_{\text{A}}m_{\text{B}})^{1/2}}.$$

The layer GF for the bicrystal, which will be used in the study of the disordered boundary, can be calculated analytically (Djafari-Rouhani *et al* 1977, Yaniv 1978, Economou 1983) and the result reads

$$G_{\text{AA}}(n, n') = P_{\text{A}}(n - n') + P_{\text{A}}(n + n' - 1) \\ + \frac{\lambda_{\text{IF}} [P_{\text{A}}(n - 1) + P_{\text{A}}(n)][P_{\text{A}}(n' - 1) + P_{\text{A}}(n')]}{m_{\text{A}} D} \\ G_{\text{AB}}(n, n') = \frac{-\lambda_{\text{IF}} [P_{\text{A}}(n - 1) + P_{\text{A}}(n)][P_{\text{B}}(n' - 1) + P_{\text{B}}(n')]}{(m_{\text{A}}m_{\text{B}})^{1/2} D} \\ G_{\text{BA}}(n, n') = \frac{-\lambda_{\text{IF}} [P_{\text{B}}(n - 1) + P_{\text{B}}(n)][P_{\text{A}}(n' - 1) + P_{\text{A}}(n')]}{(m_{\text{A}}m_{\text{B}})^{1/2} D} \\ G_{\text{BB}}(n, n') = P_{\text{B}}(n - n') + P_{\text{B}}(n + n' - 1) \\ + \frac{\lambda_{\text{IF}} [P_{\text{B}}(n - 1) + P_{\text{B}}(n)][P_{\text{B}}(n' - 1) + P_{\text{B}}(n')]}{m_{\text{B}} D}$$

where crystal A occupies the subspace $n \leq 0$ and crystal B the subspace $n \geq 1$; P_{A} and P_{B} are the perfect-crystal GF given by

$$P(n, n'; k_{\text{p}}; z) = \frac{m \tau^{|n-n'|+1}}{\lambda \tau^2 - 1} = P(n - n') \\ \tau = \sigma - (\sigma^2 - 1)^{1/2} \quad \sigma = -\frac{z}{2\lambda/m} + 3 - \cos k_x - \cos k_y$$

and

$$D = 1 - \frac{\lambda_{\text{IF}}}{m_{\text{A}}} [P_{\text{A}}(0) + P_{\text{A}}(1)] - \frac{\lambda_{\text{IF}}}{m_{\text{B}}} [P_{\text{B}}(0) + P_{\text{B}}(1)]$$

with $z = \omega^2 + i\epsilon$ and $\epsilon \rightarrow 0^+$.

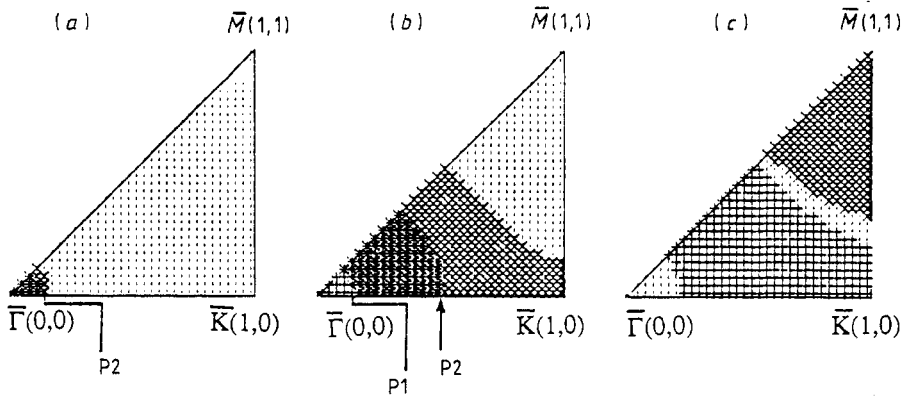


Figure 3. Projected isofrequency surfaces in the irreducible part of the surface BZ: (a) $\omega^2 = 0.14$, (b) $\omega^2 = 2.1$, (c) $\omega^2 = 4.48$; (+) crystal A, (x) crystal B.

3.2. Numerical results

The following choice of parameters was made for the interface system:

$$m_B/m_A = 2$$

$$\lambda_B/\lambda_A = \lambda_{IF}/\lambda_A = 1$$

which determines the maximum frequencies (bandwidth), in arbitrary units,

$$\omega_A^2 = 12 \quad \text{and} \quad \omega_B^2 = 6.$$

Further on, we express our results in terms of the angles defining the scattered phonon propagation direction

$$\theta = \tan^{-1} \left(\frac{(k_x^2 + k_y^2)^{1/2}}{k_z} \right) \quad \text{and} \quad \varphi = \tan^{-1} \left(\frac{k_y}{k_x} \right)$$

the symbols θ_0 and φ_0 are the corresponding angles for the incident phonon. As one would expect on physical grounds, the θ and θ_0 dependence of the cross sections is much stronger than the φ and φ_0 dependence. Therefore, the latter will be treated as parameters in the graphs below.

The calculation of the diffuse flux requires knowledge of the isofrequency surfaces (IS) of the two crystals. The projection (PIS) of those surfaces on the irreducible part of the 2D BZ (IBZ) is shown in figure 3 for three frequency values. The overlap of the PIS of the two crystals is a necessary condition for the existence of the coherent component of the transmitted field.

The angular distribution of the diffuse flux is shown in figure 4 for three different values of the concentration of B atoms. The calculation was done with 528 points in the IBZ. The main features are the following.

(i) It vanishes at large scattering angles, which is a result of the multiple scattering events in the disordered region. The same behaviour has been reported for elastic waves scattered at macroscopically rough surfaces (Ogilvy 1987).

(ii) For low frequencies the diffuse scattering shows symmetric behaviour around the case of maximum disorder, that is $r^d, t^d \propto c(c-1)$; this behaviour is characteristic

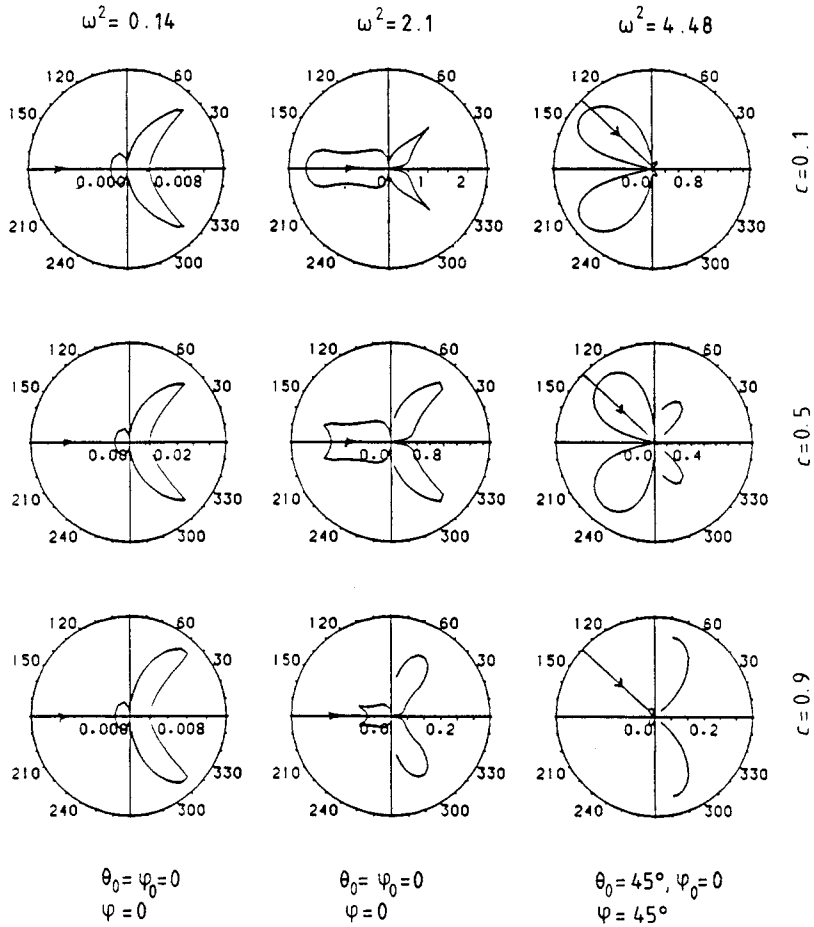


Figure 4. Angular distribution of diffuse flux; the perpendicular axis corresponds to the interface plane; the arrows indicate the propagation direction of the incident phonon.

of a weakly scattering system (Elliott *et al* 1974) and it disappears for frequencies in the dispersive regime.

(iii) As the frequency increases the scattering at large scattering angles becomes dominant, thus forming an ‘empty cone’ in the normal to the boundary direction (Schiff 1955). Notice that this ‘cone’ is always centred around the normal to the boundary direction irrespective of the direction of the incident wave, which is consistent with the interface defects acting as spherically radiating centres.

(iv) The sharp discontinuities occurring in the reflection channel ($\omega^2 = 2.1$) are associated with wavevectors that correspond to a band edge in the transmitting side. This point is indicated by P1 in figure 3. For frequencies at which the PIS do not overlap, these discontinuities do not occur ($\omega^2 = 4.48$). Similar features can be seen in the transmission channel and correspond to band edges in the reflection side ($\omega^2 = 0.14, 2.1$ and P2 in figure 3).

For a given incident phonon (ω, \mathbf{k}), we show the power reflection/transmission coefficients in figure 5. The same set of points in the IBZ as for the angular distribution

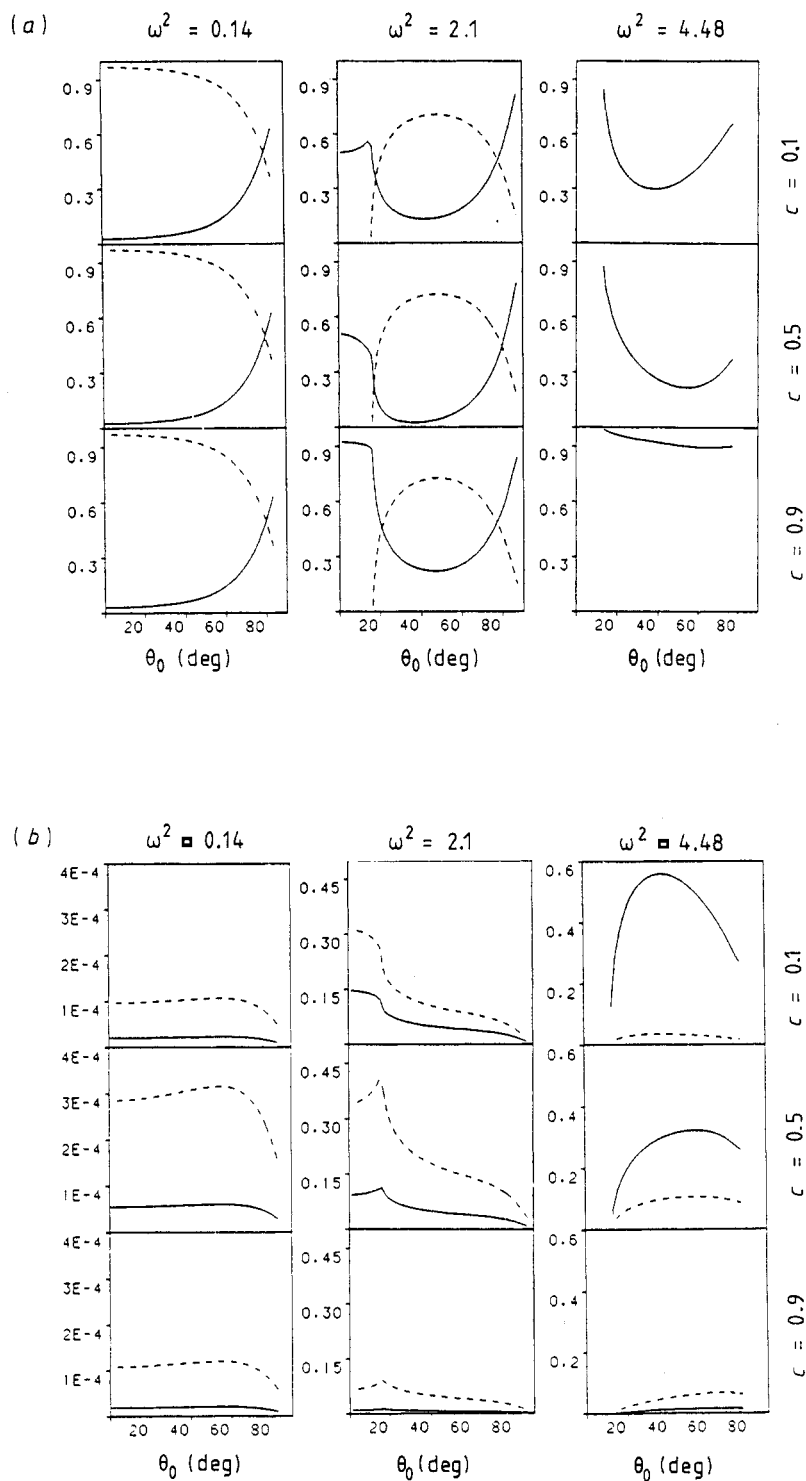


Figure 5. Power coefficients: (a) specular, (b) diffuse; full curve: reflection; broken curve: transmission; in all cases $\varphi_0 = 0$.

has been used. The flux conservation was used as a test of our calculation and it was satisfied within $\sim 1\%$. The leading features are as follows.

(i) The opening of the specular transmission channel is accompanied by a discontinuous change in the other three channels ($\omega^2 = 2.1$).

(ii) For all frequencies, the specular reflection increases with the angle of incidence at the expense of all the other channels and in the limit of grazing incidence ($\theta_0 = 90^\circ$) it becomes equal to unity; this is again a result of the multiple scattering off the total potential.

(iii) For low frequencies ($\omega^2 = 0.14$) and small angles of incidence all the scattering channels appear almost independent of the angle of incidence.

(iv) For low frequencies the diffuse channels carry only $\sim 10^{-5}$ of the total flux, while at higher frequencies up to ~ 1 , since the impurities scatter more the waves with wavelength of the order of their size ($\sim a$).

(v) For low frequencies the diffuse channels show a $\sim c(c - 1)$ dependence.

(vi) For frequencies in the dispersive region ($\omega^2 = 2.1$ and 4.48) the specular reflection is mostly sensitive to the impurity concentration and can vanish for certain values of the parameters (ω , k , c), directing the flux mainly in the diffuse channel.

(vii) For frequencies in the dispersive region the diffuse transmission channel can carry a substantial amount of flux for certain values of the impurity concentration, while the specular transmission channel is very little affected by this parameter; consequently, the total transmitted flux is enhanced by the interface microscopic roughness. This aspect of our model is in qualitative agreement with experimental evidence on the role of interface roughness in the heat transfer process between two solids (Anderson 1981).

4. Conclusions

We have suggested a lattice dynamics formalism for the phonon elastic scattering at crystal interfaces, which is based on t -matrix scattering theory and includes in a transparent way the effects of interface disorder. We have attributed the coherent scattering process to the underlying effective interface potential, which we have calculated within the CPA, and the incoherent process to the fluctuations away from the effective medium. The formalism was developed for a single-phonon-branch model and an application was made to a simple cubic interface. In the long-wavelength limit our results for disordered interfaces were in agreement with the elasticity theory predictions for random boundaries. In the dispersive region certain features remained unchanged, such as the total specular reflection at grazing incidence and the vanishing diffuse flux in directions parallel to the boundary; however, new features occurred, such as the strong ω dependence of the cross sections, cut-off angles dictated by the frequency conservation, and discontinuous changes of the cross sections with the angle of incidence, which were associated with scattering at phonon band edges.

The sensitivity of our results to the assumption of mass disorder (single-site approximation) is not important, as far as the CPA is a valid approximation in describing the vibrational properties of the interface alloy. One can go beyond the single-site approximation and consider force-constant changes or clustering effects. The formalism will remain basically the same except that the T^T matrix becomes site *non*-diagonal and equation (A2.1) should then include a summation over the sites directly coupled to the embedded defect. The limitations to this extension are imposed by the theory of random

alloys beyond the CPA (Elliott *et al* 1974, Economou 1983) rather than our *t*-matrix formulation of the boundary scattering problem.

For an extension to a multibranch model, the formal aspects of our scheme, as these are expressed by equations (1)–(4) for a clean interface and equations (11)–(18) for a disordered one, remain unchanged, but (i) the fields and the various operators should be understood as matrices of the three Cartesian coordinates, the (ii) a phonon branch index is needed to characterise the incident and scattered phonons. In this case, the lack of an analytic expression for the phonon dispersion relation increases the computational effort as an efficient procedure must be implemented to determine accurately the isofrequent points.

Finally, knowledge of the transmission cross section can provide an estimate of the related thermal boundary resistance, while the same formalism can be used for other excitations such as electrons in a tight-binding description or magnons. Work in these directions is now in progress.

Acknowledgment

I would like to thank Professor R J Elliott for pointing out this interesting problem to me and for his help and encouragement throughout the work.

Appendix 1

The Green function for a perfect crystal with a single phonon branch reads

$$P(n, n'; \mathbf{k}_p; \omega^2) = \frac{1}{N_\perp} \sum_q \frac{\exp[iq(n - n')d]}{\omega^2 - \omega^2(\mathbf{k}) + i\epsilon}$$

where $\mathbf{k} = (\mathbf{k}_p, q)$, n and n' are plane indices and $\epsilon \rightarrow 0^+$. Using the identity

$$\frac{1}{\omega^2 - \omega^2(\mathbf{k}) + i\epsilon} = -i \int_0^\infty dt \exp\{it[\omega^2 - \omega^2(\mathbf{k})] - \epsilon t\}$$

we obtain

$$P(n, n'; \mathbf{k}_p; \omega^2) = -i \frac{L_z}{2\pi} \int_{\text{1DBZ}} dq \int_0^\infty dt \exp[iF(q, t; n - n')] \quad (\text{A1.1})$$

where we have replaced the sum over the Brillouin zone with an integral, and

$$F(q, t; n - n') = q(n - n')d + t[\omega^2 - \omega^2(\mathbf{k})].$$

The stationary-phase method (Erdelyi 1956) tells us that the main contribution to the integral in (A1.1) as $|n - n'| \rightarrow \infty$ comes from the points where the phase function F is stationary

$$\begin{aligned} \partial F / \partial t = 0 & \quad \Rightarrow \quad \omega = \omega(\mathbf{k}) \\ \partial F / \partial q = 0 & \quad \Rightarrow \quad d(n - n') = 2t \omega(\mathbf{k}) \partial \omega / \partial q. \end{aligned}$$

The solutions to the last two equations are the stationary points (t^s, q^s). For a single-branch model only one stationary point exists. Note that not all the isofrequent points

are stationary, since they fail to satisfy the second of the above equations, which indicates the correct propagation direction. Expand F around the stationary point (t^s, q^s)

$$F(q, t) = q^s(n - n')d + \tau\kappa \left(-\frac{\partial\omega^2(\mathbf{k})}{\partial q} \right)_s + \frac{1}{2}\kappa^2(-t^s) \left(\frac{\partial^2\omega^2(\mathbf{k})}{\partial q^2} \right)_s + O(\kappa^2)$$

where $\tau = t - t^s$ and $\kappa = q - q^s$. Since the main contribution to the integral in equation (A1.1) comes from the region around the stationary points, i.e. $\tau = 0$ and $\kappa = 0$, we can use the approximations

$$\int_{\text{IDBZ}} dq \sim \int_{-\infty}^{+\infty} d\kappa$$

$$\int_0^\infty dt \sim \int_{-\infty}^{+\infty} d\tau$$

to obtain from equation (A1.1)

$$P(n, n'; k_p(\omega^2)) \underset{|n-n'|\rightarrow\infty}{\sim} \frac{-i}{2\pi} \exp[iq^s(n - n')d] f(s)$$

$$f(s) = \int_{-\infty}^{+\infty} d\kappa \int_{-\infty}^{+\infty} d\tau \exp \left[-i\tau\kappa \left(-\frac{\partial\omega^2(\mathbf{k})}{\partial q} \right)_s - \frac{it_s\kappa^2}{2} \left(\frac{\partial^2\omega^2(\mathbf{k})}{\partial q^2} \right)_s \right].$$

the integral factor $f(s)$ can be calculated easily and the final answer is

$$f(s) = \frac{2\pi}{|\partial\omega^2(\mathbf{k})/\partial q|_s}.$$

Therefore, the asymptotic expansion for P reads

$$P(n, n'; k_p; \omega^2) \underset{|n-n'|\rightarrow\infty}{\sim} -i \frac{\exp[iq^s(n - n')d]}{|\partial\omega^2(\mathbf{k})/\partial q|_s}. \tag{A1.2}$$

Appendix 2

The diffuse field is given by

$$\begin{bmatrix} u_A^f \\ u_B^f \end{bmatrix} = \begin{bmatrix} \bar{G}_{AA} & \bar{G}_{AB} \\ \bar{G}_{BA} & \bar{G}_{BB} \end{bmatrix} \begin{bmatrix} T^f & 0 \\ 0 & 0 \end{bmatrix} \begin{bmatrix} \bar{u}_A \\ \bar{u}_B \end{bmatrix}$$

or explicitly

$$u_A^f = \bar{G}_{AA} T^f \bar{u}_A$$

$$u_B^f = \bar{G}_{BA} T^f \bar{u}_A$$

with

$$\bar{G}_{AA} = P_A + P_A \bar{T}_{AA} P_{AA}$$

$$\bar{G}_{BA} = P_B \bar{T}_{BA} P_A$$

$$u_A = u_A^0 + P_A \bar{T}_{AA} u_A^0.$$

We proceed with the reflected field (side A). For the case of diagonal disorder the T^f matrix is site-diagonal. Furthermore, because the scattering centres of the fluctuation potential are statistically independent we only consider the scattering off the central one at $l = \mathbf{0}$. The diffuse reflected field in the site representation reads

$$u_A^f(l) = G_{AA}(l, \mathbf{0}) t^f u_A(\mathbf{0}) \quad (\text{A2.1})$$

where

$$t^f = V^f \left(1 - V^f \frac{1}{N_p} \sum_{k_p} G_{AA}(0, 0; k_p) \right)^{-1}. \quad (\text{A2.2})$$

Expand the local effective interface GF in a Fourier series

$$\bar{G}_{AA}(l, \mathbf{0}) = \frac{1}{N_p} \sum_{k_p} \bar{G}_{AA}(l, \mathbf{0}; k_p) \exp(ik_p \cdot l_p)$$

where $l = (l_p, ld)$ and the expansion coefficients satisfy Dyson's equation in the layer representation

$$\bar{G}_{AA}(l, 0) = P_A(l, 0) + \sum_{l', l''} P_A(l, l') \bar{T}_{AA}(l', l'') P_A(l'', 0) \quad k_p = \text{fixed.}$$

In the limit $|l| \rightarrow \infty$, using the results of appendix 1, we obtain

$$G_{AA}(l, 0) \underset{|l| \rightarrow \infty}{\sim} -iF_A(s) \exp(iq^s ld) \left(1 + \sum_{l', l''} \exp(-iq^s l' d) \bar{T}_{AA}(l', l'') P_A(l'' - m) \right) \quad (\text{A2.3})$$

and

$$F_A(s) = \frac{1}{|\partial \omega_A^2(\mathbf{k}) / \partial q|_s} \quad s = s(\mathbf{k}_p).$$

Furthermore, the coherent field reads

$$\bar{u}_A(\mathbf{0}) = u_A^0(0; \mathbf{k}_p^0) + \sum_{l', l''} P_A(0, l'; \mathbf{k}_p^0) T_{AA}(l', l''; \mathbf{k}_p^0) u_A^0(l''; \mathbf{k}_p^0) \quad (\text{A2.4a})$$

where the incident wave is given by

$$u_A^0(m; \mathbf{k}_p^0) = \exp(iq^0 md). \quad (\text{A2.4b})$$

Substitute equations (A2.3) and (A2.4) into equation (A2.1) to obtain

$$u_A^f(l) \underset{|l| \rightarrow \infty}{\sim} \sum_{k_p} h_A(k_p^0 \rightarrow k_p) \exp(ik \cdot l) \quad k = (l_p, q^s)$$

with the reflection amplitude given by

$$h_A(k_p^0 \rightarrow k_p) = \frac{1}{N_p} g_A(k_p) t^f \bar{u}_A(\mathbf{0})$$

$$g_A(k_p) = -iF_A(s) \left(1 + \sum_{l', l''} \exp(-iq^s l' d) \bar{T}_{AA}(l', l''; k_p) P_A(l'', 0; k_p) \right)$$

and the coherent field given from equation (A2.4).

A similar procedure is followed for the transmitted field. The final answer reads

$$h_B(\mathbf{k}_p^0 \rightarrow \mathbf{k}_p) = \frac{1}{N_p} g_B(\mathbf{k}_p) t^f \bar{u}_A(\mathbf{0})$$

$$g_B(\mathbf{k}_p) = -iF_B(s) \sum_{l', l''} \exp(-iq^s l' d) \bar{T}_{BA}(l', l''; \mathbf{k}_p) P_A(l'', 0; \mathbf{k}_p).$$

The configurational averages are given by

$$\langle h_A \rangle, \langle h_B \rangle \sim \langle t^f \rangle = 0$$

$$\langle |h_A|^2 \rangle, \langle |h_B|^2 \rangle \sim \langle |t^f|^2 \rangle = (1 - c)|t_A|^2 + c|t_B|^2$$

where t_A (t_B) is the matrix element of T_A (T_B) defined in equation (12).

References

- Anderson A C 1981 *Nonequilibrium Superconductivity, Phonons and Kapitza Resistance* (New York: Plenum)
- Arimitsu N, Paranjape B V and March N H 1984 *Solid State Commun.* **52** 399
- Chen A B 1973 *Phys. Rev. B* **7** 2230
- Deans M and Inkson J C 1989 *Semicond. Sci. Tech.* **4** 138
- Djafari-Rouhani B, Masri P and Dobrzynski L 1977 *Phys. Rev. B* **15** 5690
- Economou E N 1983 *Green's Functions in Quantum Physics* (Berlin: Springer)
- Elliott R J, Krumhansl J and Leath P L 1974 *Rev. Mod. Phys.* **46** 465
- Erdelyi A 1956 *Asymptotic Expansions* (New York: Dover)
- Jex H 1986 *Z. Phys. B* **63** 91
- Montroll E W and Potts R B 1956 *Phys. Rev. B* **102** 72
- Ogilvy J 1987 *Rep. Prog. Phys.* **50** 1553
- Pollman J and Pantelides S 1980 *Phys. Rev. B* **18** 5524
- Schiff L 1955 *Quantum Mechanics* (New York: McGraw-Hill)
- Steinbrüchel C 1976 *Z. Phys. B* **24** 293
- Streib H M and Mahler G 1987 *Z. Phys. B* **565** 483
- Wybourne N M and Wigmore J K 1988 *Rep. Prog. Phys.* **51** 923
- Yaniv A 1978 *Phys. Rev. B* **17** 3904